Supporting Text

Calculation of B-DNA Twist/Stretch Coupling Constant. The energy of DNA per unit length, in the linear response limit, can be approximated as

$$E/L_0 = \frac{4\pi^2 k_B T}{p^2}(C\sigma^2 + B\epsilon^2 + 2D\epsilon\sigma), \tag{1}$$

where $\epsilon = L/L_0 - 1$ is the relative change in extension L, $\sigma = Tw/Tw_0 - 1$ is the relative change in twist Tw, $p = 3.6$ nm is the DNA pitch, and $C = 100$ nm, $B = 78$ nm represent the torsional, and, respectively, stretch moduli for DNA (with values from reference [1]). D is the twist-stretch coupling constant we seek to compute from our simulations.

The average DNA structure created in each umbrella sampling window that had an RMS > 9.5 Å (i.e., within a linear-response, small twist-angle region of up to approximately 2 Å away from B-DNA) was analyzed with CURVES 5.0 [2] to determine the extension and twist of the central 6 base pairs. The coupling constant D was determined by fitting the numerical extension-twist dependence (see Fig. 1 below) to the equation:

$$\epsilon - \epsilon_{\sigma=0} = -D\sigma/B, \tag{2}$$

where L_0 and Tw_0 are the equilibrium extension and twist, determined from the $\rho = 11.5$ Å window (the canonical B-DNA form, with values 3.43 nm and 35.18°, respectively). The value of $\epsilon_{\sigma=0}$ was derived from a linear fit of ϵ vs. σ values (giving $\epsilon_{\sigma=0} = 0.0152$). Averaging of all ϵ values determined by this method gives $D = -15.4 \pm 53.5$ nm.

Although the variance is large (because of the small, finite size of the system, relative fluctuations do not decay sufficiently) the negative character of twist-stretch coupling is indisputable (see Figure 1 below). The

average coupling constant $D = -15.4$ nm compares favorably with the result of Lionnet *et al.*, who report $D = -9.1 \pm 4$ nm, and with that of Gore *et al.* [3], who measure $D = -11.1 \pm 2.5$ nm. (The value for the coupling constant $g = -90$pN·nm reported by Gore *et al.* was transformed to D, i.e., in the units used by Lionnet *et al.*, by employing the formula $g/S = Dp/(2\pi B)$ with $S = 1,100$ pN the stretch modulus used in Gore *et al.*)

It is also worth noting that our calculated value is close to those reported in the modeling section of the Lionnet *et al.* reference, who computed, using a different force field (see ref. [4] therein) and helical-symmetry energy minimization, values of $D = -13$ to $D = -20$ nm, depending on the applied tension.

References

[1] Lionnet T, Joubaud S, Lavery R, Bensimon D,Croquette V (2006) *Phys. Rev. Lett.* 96:178102

[2] Lavery R, Sklenar H (1988) *J. Biomol. Struct. Dyn.* 6:63-91

[3] J. Gore, Z. Bryant, M. Nöllmann, M.U. Le, N.R. Cozzarelli, C. Bustamante, *Nature* ***2006,*** *advanced online publication, doi:10.1038/nature04974*

[4] Cheatham TE, Cieplak P, Kollman PA (1999) *J. Biomol. Struct. Dyn.* 16:845

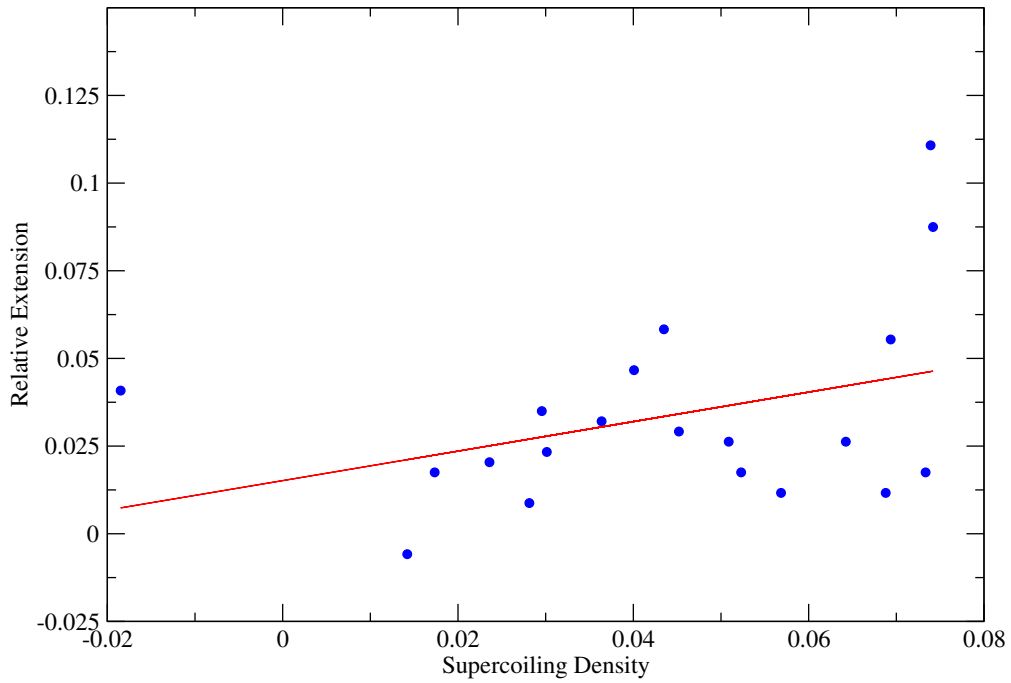

Figure 1: Twist-stretch dependence from umbrella sampling simulations (blue points) and the linear fit to Eq. (2) (red line)

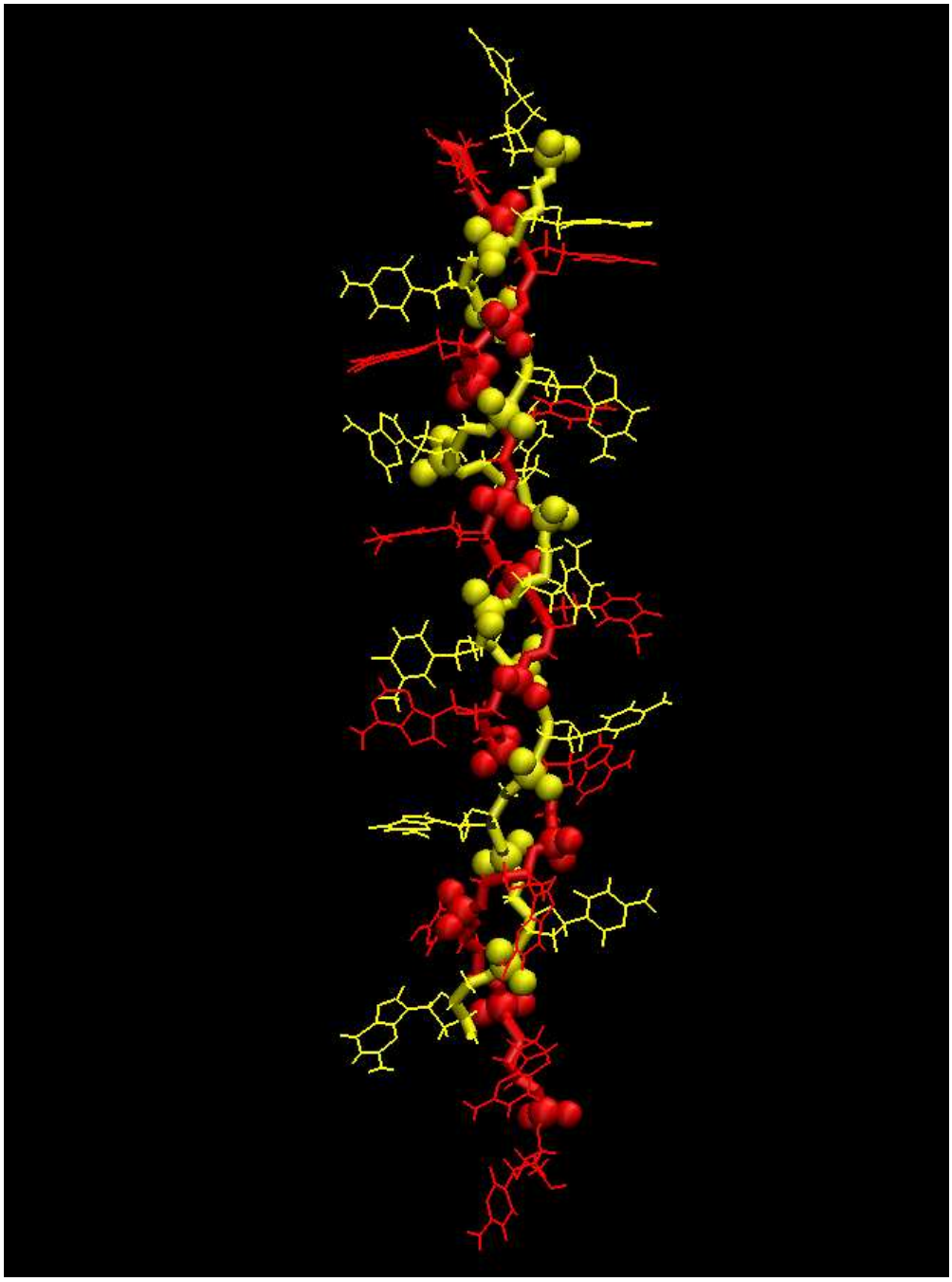

Figure 2: Atomistic view of P-DNA backbone (in bond representation). The phosphate anionic oxygens (smaller spheres) radiate outwards from the DNA axis to minimize their electrostatic interactions, while the phosphorus atoms (large spheres) on opposite strand (colored yellow or red) line up in a more staggered position than when in B-DNA. The ribose rings of both strands assume a perpendicular position relative to the helical axis. Phosphorus and anionic oxygen atoms are explicitly shown according to their van der Waals radius.

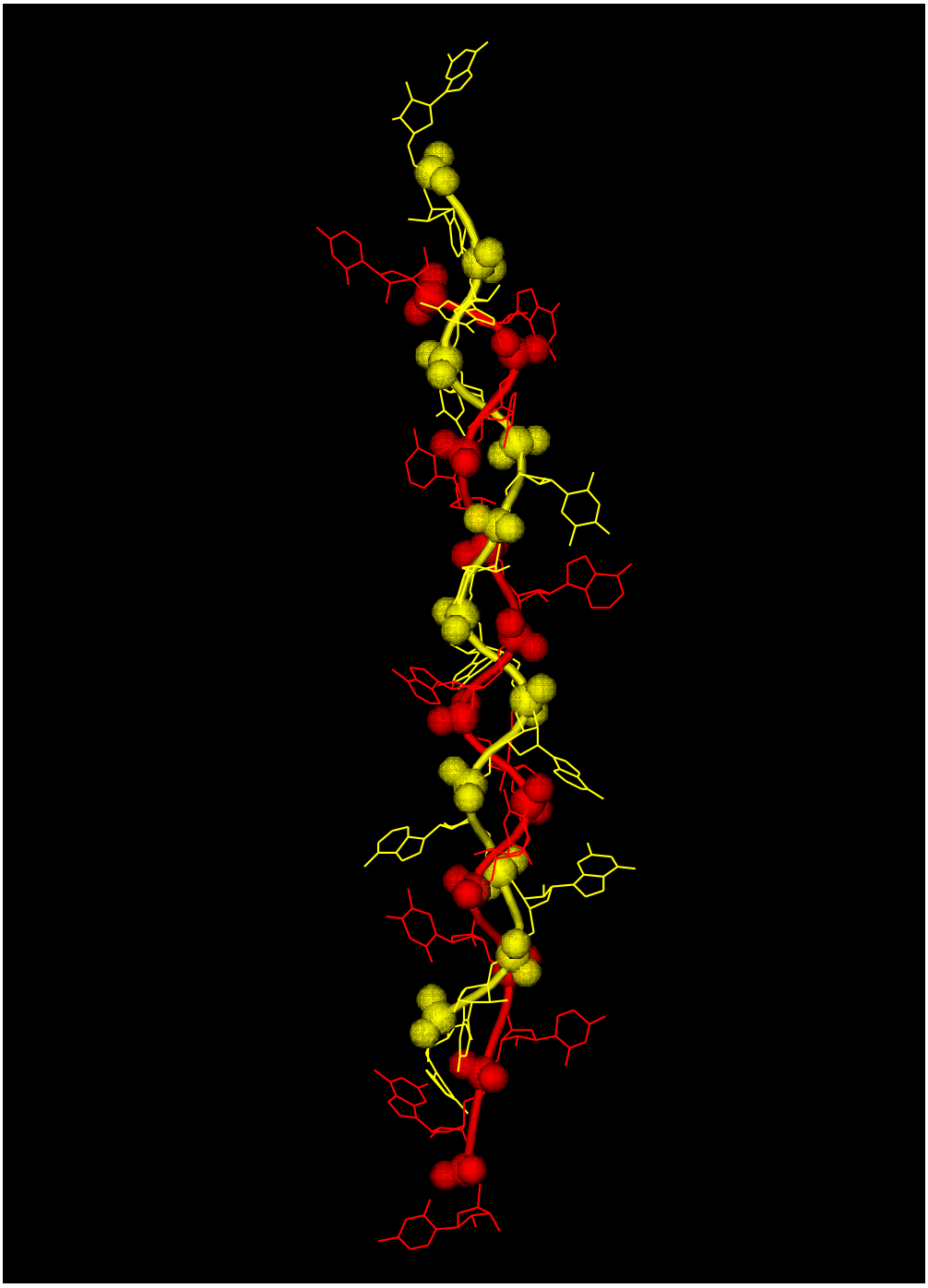

Figure 3: Atomistic view of the P-RNA backbone. Same representation as in Fig. 2

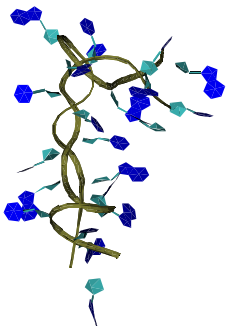

(a) Overtwisting with low tension

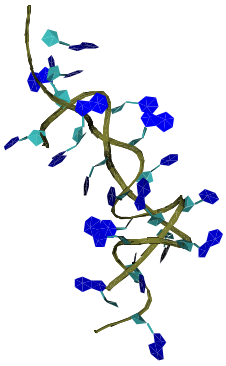

(b) Overtwisting with medium tension

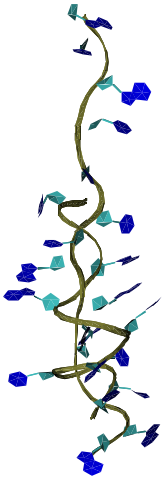

(c) Underwisting with low tension

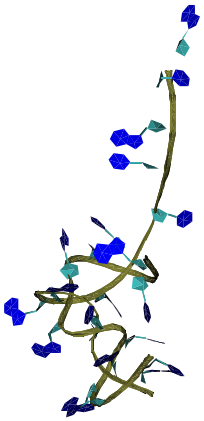

(d) Undertwisting with medium tension

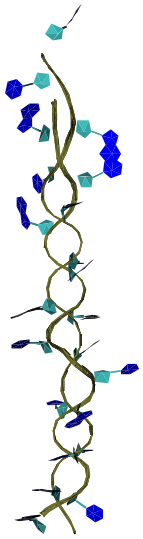

(e) Undertwisting with high tension

Figure 4: Final DNA structures created in simulations with a positive or negative driving torque and various tensions.

(a) Overtwisting with low tension

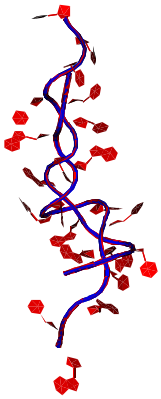

(b) Overtwisting with medium tension

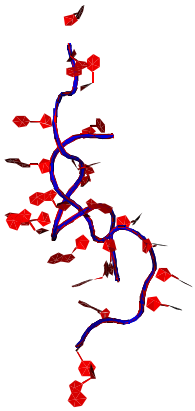

(c) Underwisting with low tension

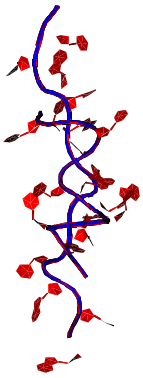

(d) Undertwisting with medium tension

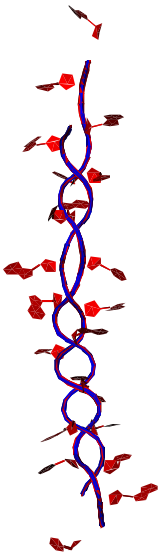

(e) Undertwisting with high tension

Figure 5: Final RNA structures created in simulations with a positive or negative driving torque and various tensions.

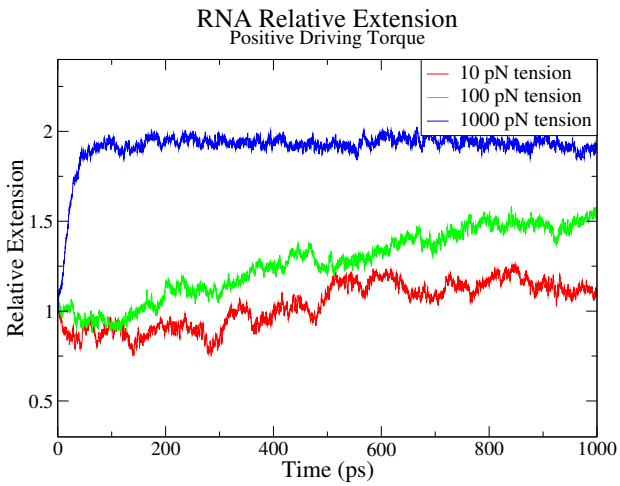

(a) Relative extension of RNA under a positive driving torque as a function of time

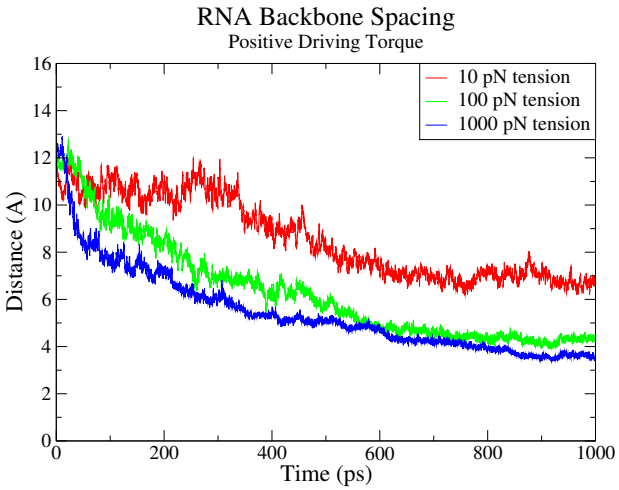

(b) Backbone spacing of RNA under a positive driving torque as a function of time

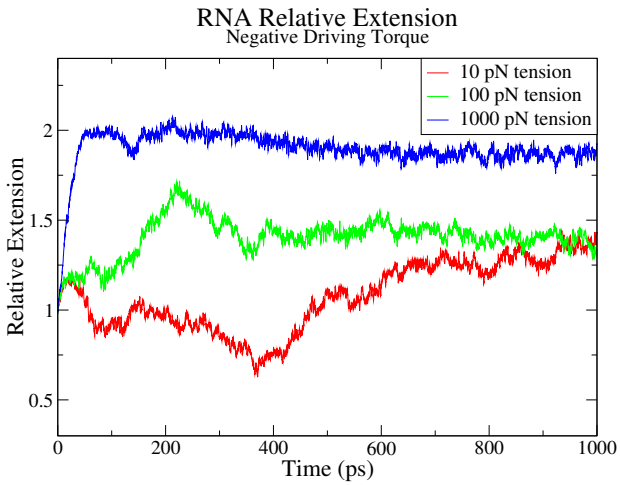

(c) Relative extension of RNA under a negative torque as a function of time

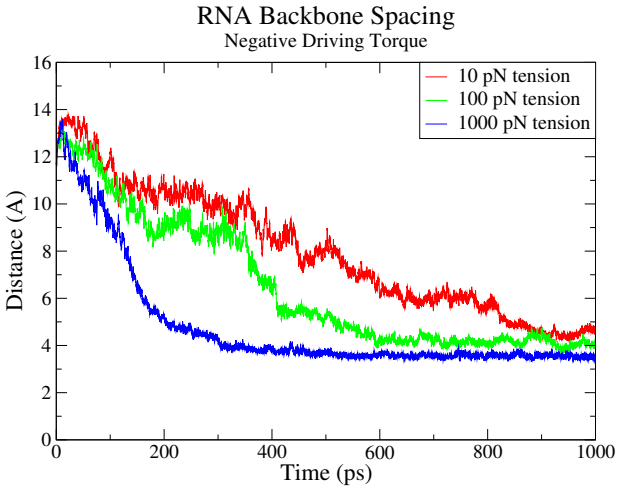

(d) Backbone spacing of RNA under a negative driving torque as a function of time

Figure 6:

Structure	α	β	γ	δ	ϵ	ζ
$B-DNA$	$-60°$	$165°$	$53°$	$132°$	$-163°$	$-112°$
$P-DNA$	$-55°$	$176°$	$-156°$	$129°$	$-168°$	$160°$
$A-RNA$	$-88°$	$172°$	$64°$	$78°$	$-156°$	$-70°$
$P-RNA$	$175°$	$180°$	$116°$	$138°$	$-168°$	$160°$

Table 1: Equilibrium backbone torsion angles ($\alpha - \zeta$) for P-form nucleic acids calculated from umbrella sampling simulations at $\rho = 1$ (see text for details).

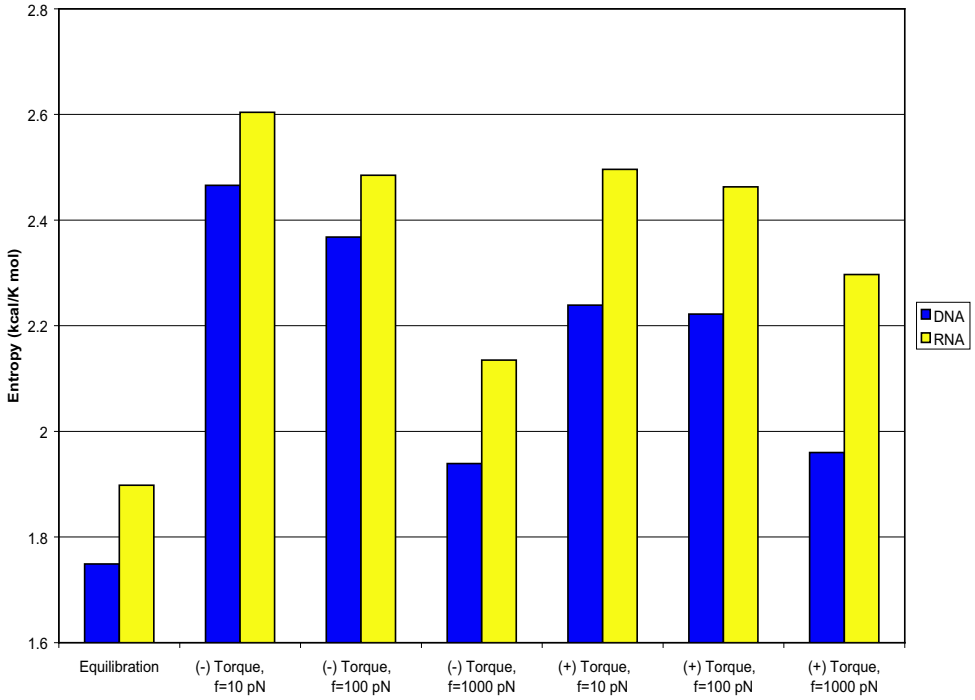

Figure 7: Conformational entropy from quasiharmonic analysis of the ten non-terminal base pairs for the various DNA and RNA structures discussed in the main text. A temperature of 300 K and a scaling factor of 12/10 (accounting for the quasi-extensivity of entropy) were used to calculate the $-T\Delta S$ values reported in Table 1 in the text.